# Metasomatism in the North Qôroq centre, South Greenland: apatite chemistry and rare-earth element transport

DAVID A. RAE, IAN M. COULSON* AND ANDREW D. CHAMBERS

School of Earth Sciences, The University of Birmingham, Edgbaston, Birmingham B15 2TT, UK

## Abstract

The North Qôroq syenite centre forms part of the Gardar Province of South Greenland. Extensive metasomatism, associated with the evolution of syenitic magmas, has resulted in redistribution of the rare-earth elements (*REE*), originally concentrated by magmatic processes, in both the syenites and surrounding granite-gneiss and quartzite country rocks. An important host for *REE* is apatite which can occur in significant quantities. Metasomatic apatites show complex, concentric, but irregular patterns of zonation, clearly seen using CL and BSE imaging. This zonation is related to successive pulses of metasomatising fluids. Electron microprobe analysis confirms the presence of significant quantities of *REE* in the apatites. The dominant cation exchange mechanism proposed is $Ca^{2+} + P^{5+} \leftrightharpoons REE^{3+} + Si^{4+}$. In contrast to apatites from the nearby Ilímaussaq intrusion, there is no significant Na present in the structure and exchange reactions involving $Na^{+}$ and $REE^{3+}$ for $Ca^{2+}$ have not occurred.

Apatites from the quartzite are fluor-apatites, while those from the granite-gneiss are more Cl-rich. These differences reflect the fact that granite-gneiss apatites are original and modified by metasomatism, whereas, those in the quartzite are metasomatic in origin. *REE* were probably transported as carbonate, fluoride or fluor-carbonate complexes, and reflect the activity of a $F^{-}$-rich, $CO_3^{2-}$-rich fluid phase.

KEYWORDS: apatite, metasomatism, rare-earth elements, cathodoluminescence, Igaliko, Gardar, South Greenland.

## Introduction

APATITE $\{Ca_5(PO_4)_3(OH,F,Cl)\}$ is present as a minor phase in almost all igneous rock types, and is a common accessory in numerous other environments (McConnell, 1973). Its structure is such that it can concentrate many trace elements, in particular the rare-earth elements (*REE*). It, therefore, has an important role in controlling the distribution of *REE* in igneous, metamorphic, metasomatic and hydrothermal processes (Roeder *et al.*, 1987; Lieftink *et al.*, 1994). A knowledge of the *REE* contents of apatites, therefore, is critical to any model dealing with the behaviour of these elements.

A combination of mineral chemistry, cathodoluminescence and back-scattered electron imagery forms the basis of this study and this paper describes the chemistry of apatites associated with the alkali metasomatism of pre-existing syenites, the basement granite-gneiss (Julianehåb Granite) and supracrustal rocks within and around the North Qôroq nepheline syenite centre.

## Geological setting

The North Qôroq centre is the smallest and most north-westerly of four syenite centres that comprise the Igaliko complex, one of a number of major complexes to be found in the Gardar Province of South Greenland (Fig. 1). Reviews of this Proterozoic alkaline province have been produced by Upton and Emeleus (1987) and Macdonald and Upton (1993). All four major centres in the Igaliko complex consist dominantly of nepheline syenites and each is made up of a number of generally concentric units. A

---

* Author for correspondence

*Mineralogical Magazine, February 1996, Vol. 60, pp. 207–220*

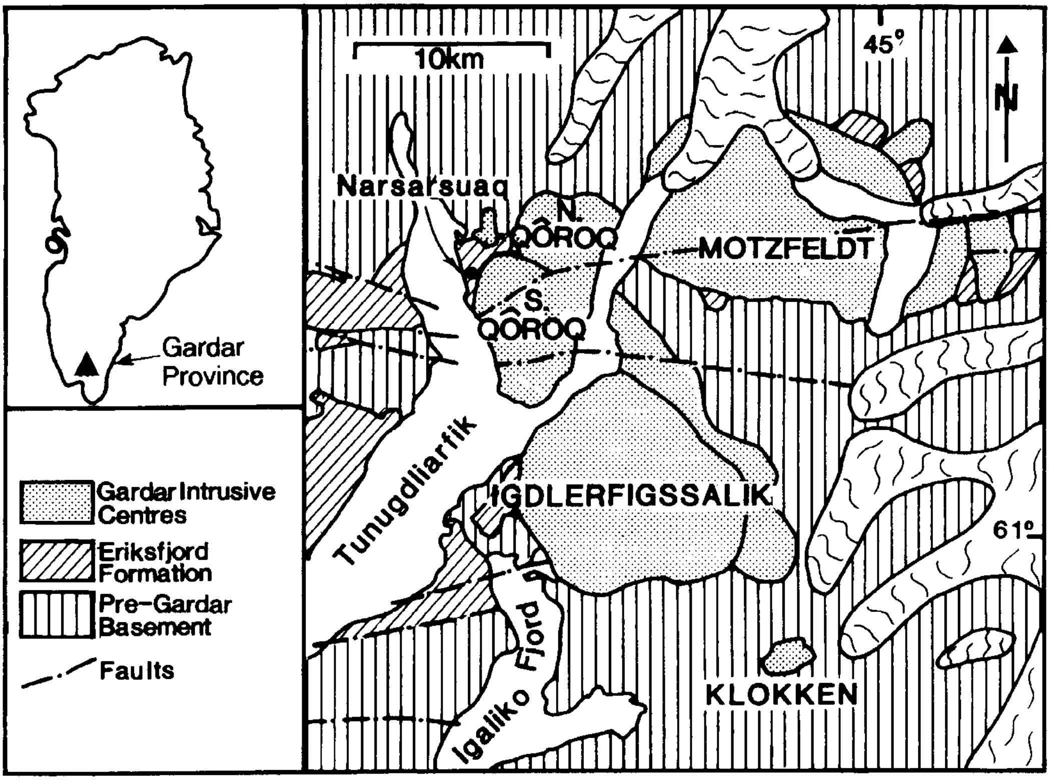

FIG. 1. Simplified map of the Igaliko nepheline syenite complex, Gardar province, South Greenland, showing the four centres: North Qôroq, South Qôroq, Motzfeldt and Igdlerfigssalik.

detailed account of the Igaliko Complex is given by Emeleus and Harry (1970).

The North Qôroq centre, dated at 1262 ± 55Ma* (Blaxland *et al.*, 1978), consists of six major units designated SN1A to SN5 in order of emplacement (Fig. 2). The syenites were intruded at a high crustal level and all display undersaturated character. Units show the effects of *in situ* fractionation with highly fractionated and peralkaline cores. Extensive fluid activity appears to have played a part during the late stage evolution of the most fractionated North Qôroq syenitic magmas, resulting in metasomatism within the centre and the country rocks. Evidence suggests that fluids of more than one composition may have been active with a Na- and Cl-rich phase producing albitization, sodic pyroxene and amphibole and a Ca-, F-, $CO_3$-rich phase locally overprinting this.

To the north the centre intrudes the Ketilidian basement gneissose granites and granodiorites of the Julianehåb Granite complex. The nature of the contact varies with height in the intrusion and metasomatism is most evident in the roof zone. To the west the centre cuts early Gardar sediments and lavas. The samples of quartzite studied are included in the syenite unit SN1B (Fig. 2), as a raft, which looks to have been stoped into the syenite. The southern boundary, partially intrusive and partially faulted, is formed by the younger South Qôroq centre (1159 ± 8 Ma; Blaxland *et al.*, 1978). To the east the contacts are obscured by Qôroq fjord and the steep cliffs bounding the fjord.

These various types of country rock and syenite protolith show differences in style and degree of alteration. It appears that not only the chemical characteristics of the protolith but also the physical characteristics such as permeability and porosity play important roles in determining the course of metasomatism.

---

* data recalculated to the decay constants of Steiger and Jäger (1977)

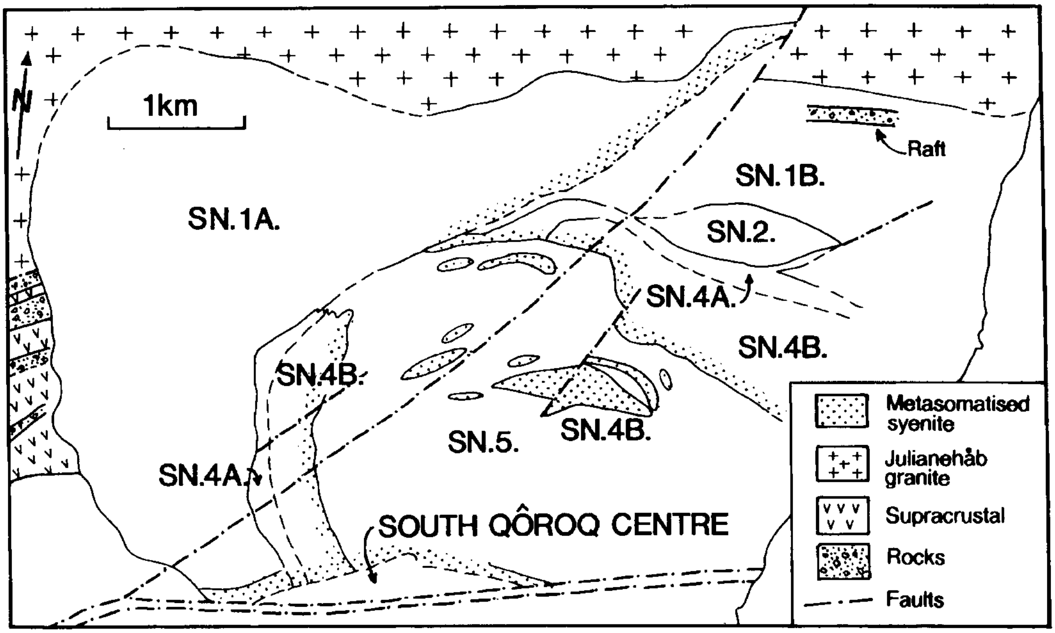

FIG. 2. Geological map of the North Qôroq centre, showing individual units constituting the centre (SN1A-SN5), the principal areas of metasomatised syenite, the granite-gneiss and the supracrustal country rocks.

## Petrography

### *The Julianehåb Granite*

The Julianehåb Granite is a two feldspar granite-gneiss. In unaltered samples microcline, partly sericitised plagioclase feldspar and strained quartz form the bulk of the mode. Biotite, amphibole, opaques and apatite are present in minor amounts. Metasomatism results in the reduction and eventual disappearance of quartz with extensive growth of brown, green or fibrous blue alkali-amphibole and large flakes of biotite. With rocks in the immediate contact zone adjacent to the syenite, extensive albitization (up to 90% modal Ab) occurs. Calcite and fluorite occur as patches and veins in the groundmass.

### *Supracrustal rocks*

Country rock basalt lavas are dark, fine grained and porphyritic in hand specimen. Microscopic study shows extensive alteration with recrystallization, veining and replacement of mafic minerals, with biotite as the dominant new phase. Apatite, sphene and zircon commonly occur as new metasomatic phases in late-stage veins in association with calcic-pyroxenes and amphiboles, opaques, calcite, white mica, fluorite, hydro-grossular garnet and occasionally tourmaline.

Metasomatised supracrustal rocks include the quartzite raft within SN1B. There appear to be two types of effect associated with the metasomatism of these rocks:

*Type 1.* Here metasomatic effects are patchy and variable. Rocks in which there is still abundant quartz show haematite coating of grain boundaries and the irregular development of laths of euhedral albite between the quartz grains. This type of alteration can progress to the formation of a fine-grained matrix dominated by albite. There is sporadic and limited growth of alkali-pyroxenes (aegirine-augite) and poikilitic or fibrous alkali-amphibole (magnesio-arfvedsonite). Apatite is absent from these albitised areas.

*Type 2.* Large clusters or pods are formed which are dominated by a mass of euhedral to subhedral aegirine-augite crystals, with less abundant amphibole. Fluorite and calcite occur as veins associated with the mafic minerals and also as interstitial patches. Apatite is disseminated throughout the mafic pods and takes the form of small equant grains in pyroxene, amphibole, calcite and fluorite. Large clusters of apatite are formed along the contacts between the pods or veins of mafic minerals and the surrounding albitised matrix, producing a

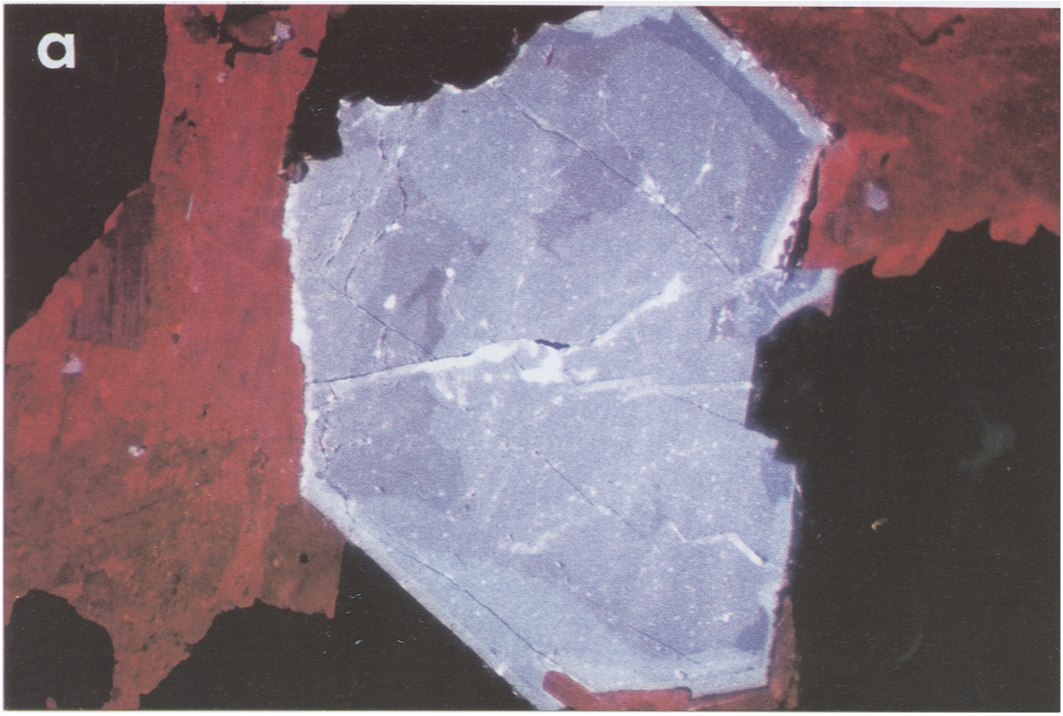
a

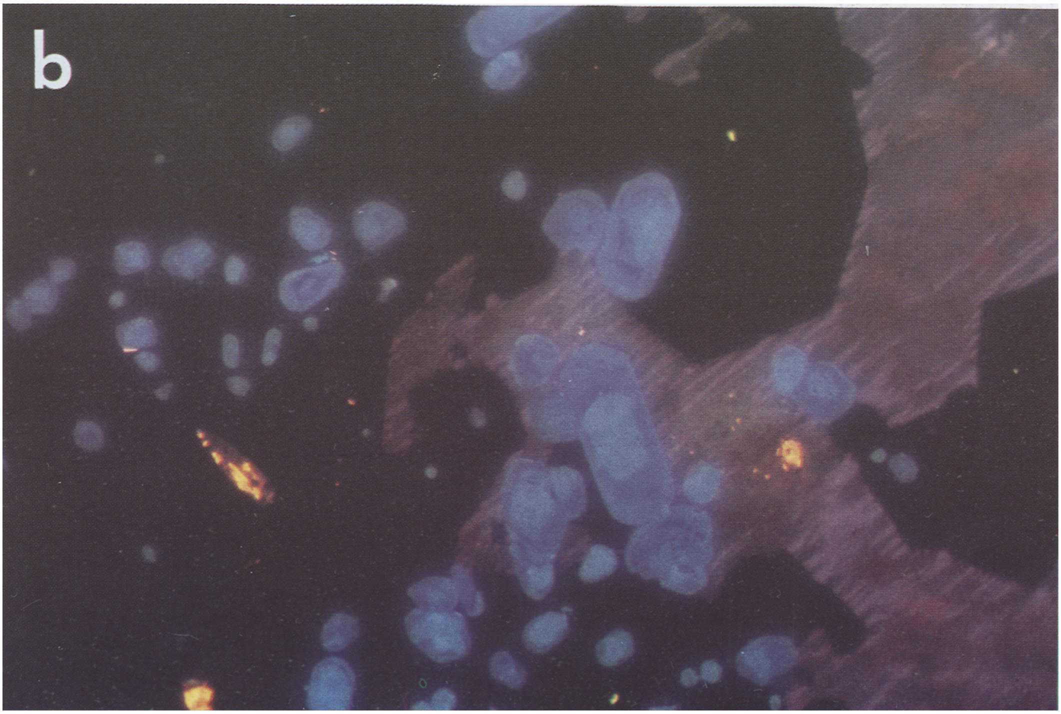
b

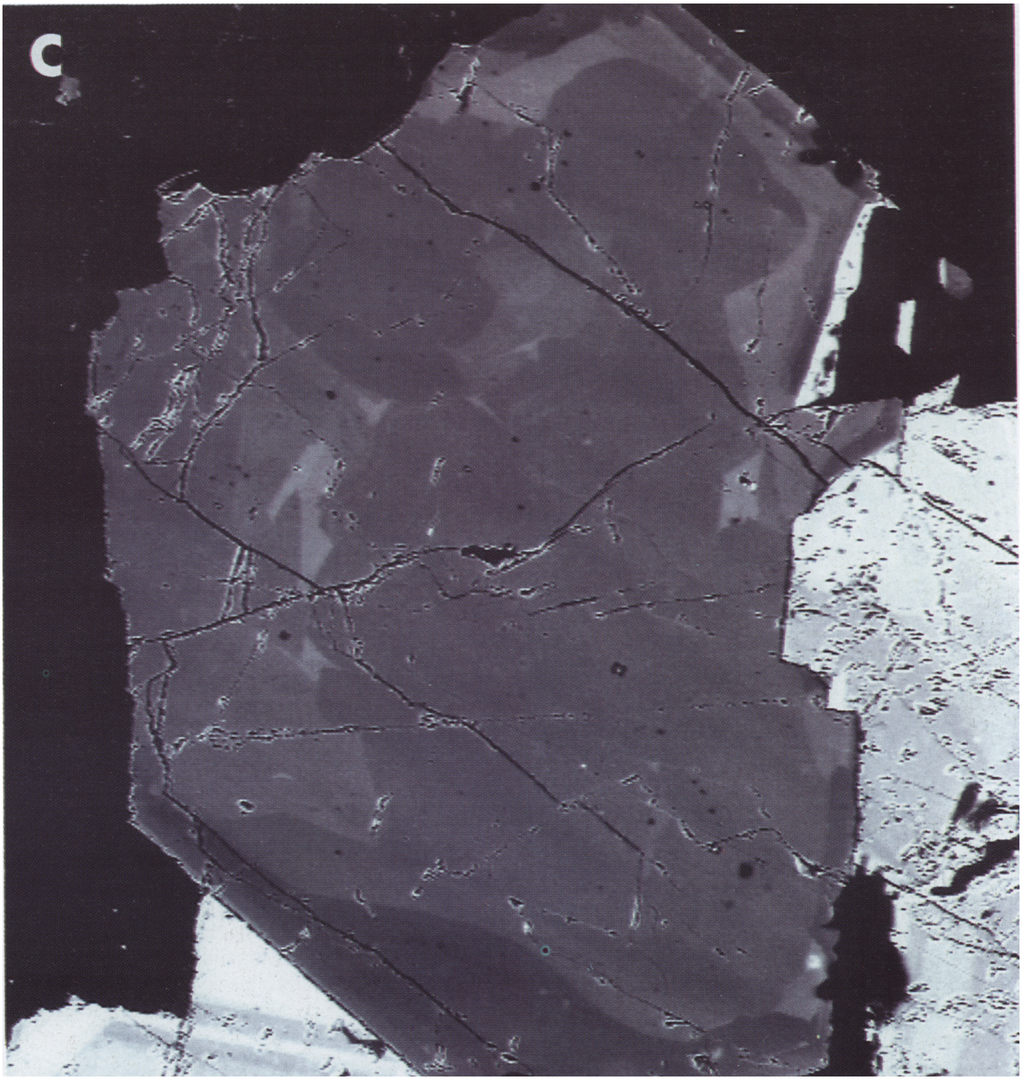

FIG. 3 (*a* and *b* opposite). Cathodoluminescence (CL) and back-scattered electron (BSE) images of North Qôroq apatites. (*a*) CL photomicrograph of complex zonation in apatite from a metasomatised evolved syenite. Red luminescing mineral is feldspar. (*b*) CL photomicrograph of smaller apatite crystals within the fenitised quartzite raft, again displaying complex zonation. Note pale pink luminescing feldspar and bright orange luminescing calcite. (*c*) BSE image of apatite in (*a*) displaying some subtleties in zonation not visible using CL. Fields of view: (*a*) and (*b*) 2.0 mm; (*c*) 0.9 mm.

thick rim of apatite between the two areas. This development of apatite is clearly restricted to areas where mafic minerals are abundant.

### *Syenites*

The samples of syenite studied are from the largest unit, SN1A (Fig. 2) which has been metasomatised both by the intrusion of the younger South Qôroq centre and by later units of North Qôroq itself. Metasomatism of the syenites produces distinctive textures in both the mafic and felsic phases, the most common of which is the development of large poikilitic crystals of aegirine-augite, alkali-amphibole and aenigmatite. The felsic mineralogy consists of nepheline, relict perthite and albite, whilst sodalite and analcite usually dominate the groundmass. Common accessories in the metasomatised syenite are calcite, cancrinite, fluorite, apatite and a rinkite-møsandrite group mineral.

## Cathodoluminescence petrography and electron imaging

### *Cathodoluminescence petrography*

Comprehensive reviews of cathodoluminescence (CL) in minerals and a discussion of the luminescence process are given by Walker (1985) and Marshall (1988).

Initial studies of CL in apatites concerned synthetic apatites (Quirk and Thomas, 1964; Palilla and O'Reilly, 1968) and work on natural apatites soon followed (Smith and Steenstrom, 1965; Portnov and Gorobets, 1969). Natural apatites were seen to luminesce in a variety of colours and the above workers stressed the importance of $Mn^{2+}$ and *REE* contents in controlling both intensity and colour.

Mariano and Ring (1975) attributed CL in apatites to Eu activation with minor effects produced by other rare-earth elements, such as Sm and Dy. They stated that $Eu^{2+}$ produced a blue luminescence that was common to apatites of carbonatites and fenites. Alternatively, blue luminescence in apatite may mainly be due to a structural defect produced by large amounts of *REE* substituting for $Ca^{2+}$ in the structure (Roeder *et al.*, 1987). The apatites in North Qôroq do not luminesce a simple blue colour but in shades of violet, blue and purple, suggesting the presence of additional activators (possibly $Eu^{3+}$, Portnov and Gorobets, 1969; Voron'ko *et al.*, 1992).

The luminescence observed in North Qôroq apatites contrasts with the majority of adjacent Gardar centres, where apatites luminesce in shades of orange, mauve and canary yellow (Finch, 1990), although in a few samples from the Motzfeldt and South Qôroq centres blue-luminescent apatite is seen. Hayward and Jones (1991) studied apatites from the nearby extrusive carbonatite at Qasiarsuk and found both blue and violet luminescing apatite, similar to those seen in North Qôroq. They suggested that the blue luminescing apatite cores were produced by $Eu^{2+}$ activation (magmatic), whereas the violet apatite rims were produced by $Eu^{2+}$ and $Eu^{3+}$ activation, representing overgrowth in oxidising conditions (magmatic and hydrothermal).

The details of variations in apatite CL are probably very complex and it is only the basic supposition that variations in luminescent colour are a result of variations in *REE* contents that is of prime importance. This hypothesis is supported by data from a detailed electron micro-probe (EPMA) study.

Standard optical microscopy does not reveal any detail in the apatites. CL microscopy, however, reveals a more complex and variable pattern. Apatites from syenites apparently unaffected by metasomatism are unzoned or show systematic sector zonation consistent with growth mechanisms involving crystallization from a primary magma. Apatites from the metasomatised rocks, however, show much more complex relationships. In the granite-gneiss and basalt, metasomatised apatites commonly only have a simple blue core and darker purple outer rim, whereas apatites from the quartzite raft and syenites show more complex zonation. Here up to five irregular concentric zones, luminescing with different intensities (Figs. 3*a,b*) are the result of several periods of metasomatism. Outer zones commonly cut across and embay earlier inner zones and the pattern suggests that some apatites have been affected by a series of up to five metasomatic events.

### *Electron imaging*

The apatite zonation observed using CL is also seen using back-scattered electron imagery (Fig. 3*c*). Typical BSE images of apatites from the granite-gneiss and basalts, which are adjacent to only a single syenite unit, show simple zonation with distinct dark cores and bright rims. In apatites from the quartzite raft and syenite more complex patterns are displayed. Figure 3*c* shows this more complex zonation in a metasomatised syenite sample, where later zones can be seen to truncate and embay earlier ones. Each zone appears to be internally homogeneous with sharp boundaries against adjacent zones. This pattern is characteristic of quartzite and syenite apatites, reflects multiple metasomatic events, and is due to their proximity to a number of later syenite units.

Electron imagery reveals several other rare-earth bearing minerals present in the metasomatised North Qôroq rocks. One is a member of the rinkite-møsandrite group and others include monazite, eudialyte, titanite, zircon and as yet unidentified fluor-carbonate minerals probably from the bastnäsite family (synchysite). Further work is underway to identify these unknown phases and will be presented in a later paper (Coulson *et al.*, in prep.)

## Apatite chemistry

### *Analytical techniques*

Wavelength dispersive electron microprobe analyses were carried out using a Cameca Camebax instrument. The accelerating voltage was 20 kV and the beam current varied between 20 and 25 nA with an 8K raster. Synthetic silicate glasses made at Edinburgh University were used as standards for the *REE*. The glasses are doped with between 15–20 wt.% of the appropriate *REE* oxide. The elements Ca, P, Si, Na, Sr, Ba, Fe, Mn, Mg, La, Ce, Pr, Nd, Sm, Y, F and Cl were analysed for, and representative analyses are listed in Table 1. Lanthanum, Ce, Nd and Y were analysed using $L\alpha$ lines whereas for Pr and Sm-$L\beta$ was used. Fluorine was analysed using the second order $K\alpha$ line on a PC2 synthetic multilayer crystal (100 Å 2d), so avoiding third order P-$K\alpha$ interference, and higher order interferences were removed using pulse height discrimination. Samples exposed to an electron beam from cathodoluminescence studies were repolished before analysis (Stormer *et al.*, 1993). As a guide to analytical accuracy, a sample of homogeneous apatite from Durango, Mexico (Young *et al.*, 1969) was analysed by the same technique and the results were found to be consistent with recommended values (Reed, 1986).

### *Cation element variation*

Table 1 gives typical metasomatic apatite analyses obtained from all protolith types; granite-gneiss, quartzite, basalt and syenite. Cores, inner rims and outer rims of crystals are indicated in the table. The Ca and P content of North Qôroq metasomatic apatites show significant variation from that for the pure end-member and this is related to extensive substitutions occurring in the apatite lattice. The variation is shown in Fig. 4 where major and minor oxides are plotted against CaO. Apatites from all metasomatised rock types show significant compositional range with this being most pronounced in the quartzite raft, where total $RE_2O_3$ can reach 10.4 wt.%.

It can be seen from Fig. 4 that as CaO decreases, $P_2O_5$ also decreases and $SiO_2$ and $RE_2O_3$ ($Ce_2O_3$ plotted) increase. Comparison of analyses with both the BSE and CL images (Fig. 3) demonstrates a simple relationship. Zones that luminesce purple and have a brighter BSE response are richer in *REE*s, whereas, blue luminescing dull zones have lower concentrations.

Of the minor elements only Sr occurs in significant amounts (up to 3.5 wt.% oxide). Strontium values contrast markedly, depending on the type of country rock protolith. Quartzite raft apatites show high values, normally between 1 and 3 wt.% SrO, whereas the granite-gneiss has SrO close to detection limits. Both metasomatised basalt and syenite apatites show values spanning the gap between these two. Because Sr substitutes for Ca in the apatite structure and CaO is used as abscissa all plots show minor separation, particularly of quartzite and granite-gneiss analyses.

Of the other cations analysed, only Fe and Na and rarely Mn were detected. Concentrations of Fe and Na never exceeded 0.5 wt.% oxide.

Step traverses across the apatite crystals confirm that each zone is internally homogeneous, not only in *REE* content but also in Si, Ca and Sr. More detailed treatment of the apatite zonation is deferred until the discussion section.

### *Cation substitutions*

The strong *REE* enrichment observed in the apatites raises the question of the substitutions taking place. Several authors have noted significant *REE* substitution in apatites (e.g. Henderson, 1980; Rønsbo, 1989). Watson and Green (1981) emphasise that the substitution of $REE^{3+} \leftrightharpoons Ca^{2+}$ affects the charge balance and in order to maintain this there has to be a coupled substitution involving a $^{4+}$ ion entering the $P^{5+}$ site. The correlation seen in Fig. 4 indicates that $Si^{4+}$ is substituting for $P^{5+}$ as $REE^{3+}$ substitutes for $Ca^{2+}$, with charge balance being maintained. When $Sr^{2+}$ is added to $Ca^{2+}$ the substitution $Ca^{2+}$ ($Sr^{2+}$) + $P^{5+} \leftrightharpoons REE^{3+} + Si^{4+}$ can be seen to be the dominant one and accounts for almost all the variation in apatite chemistry (Fig. 5) irrespective of protolith type. There is minor scatter in this trend and analyses lie marginally below the 1:1 line of this substitution. This is slightly more pronounced at lower (Ca + P) values and there is a suggestion that the syenite apatite analyses diverge more from the ideal line than those from the country rocks. This suggests that other very minor substitutions do occur. $2REE^{3+} + \square \leftrightharpoons 3Ca^{2+}$ is a possibility, where $\square$ is a vacancy. Such substitutions could explain slight deviation from stoichiometry seen in the analyses. Iron is likely to be present in the ferric state as the presence of $Fe^{2+}$ would have quenched the luminescence of the apatites (Filippelli and Delaney, 1993) and it too will enter a $Ca^{2+}$ site. A coupled substitution is again required and $Ca^{2+} + P^{5+} \leftrightharpoons Fe^{3+} + Si^{4+}$ is feasible.

A substitution described in apatites from similar environments to North Qôroq is $2Ca^{2+} \leftrightharpoons Na^+ + REE^{3+}$ where the Na/*REE* end-member is vitusite (Rønsbo *et al.*, 1979). This substitution scheme has been identified in a number of syenite intrusions in South Greenland belonging to the same province as North Qôroq. These include the Ilímaussaq (Rønsbo, 1989) and Igdlerfigssalik (Finch, 1990) intrusions. It has also been described from the chemically similar Lovozero massif of the Kola peninsula (Rønsbo *et al.*, 1979). Sodium contents in North Qôroq metasomatic apatites are always very low indicating that, at least in this environment, the exchange is not significant.

### *Anion element variation*

Fluorine is the dominant halide with analyses showing all the apatites to be fluor-apatite and

TABLE 1. Representative wavelength dispersive electron microprobe analyses of North Qôroq apatites

| Sample No. | DAR65 | DAR65 | DAR67 | DAR67 | DAR67 | DAR164 | DAR165 | DAR165 | DAR167 | DAR278 | DAR278 | DAR278 | DAR301 | DAR301 |
|---|---|---|---|---|---|---|---|---|---|---|---|---|---|---|
| | c | ir | ir | c | or | c | or | or | c | c | ir | or | c | or |
| | 1 | 2 | 3 | 4 | 5 | 6 | 7 | 8 | 9 | 10 | 11 | 12 | 13 | 14 |
| CaO | 50.48 | 49.79 | 47.98 | 51.84 | 50.57 | 55.14 | 53.90 | 54.21 | 54.34 | 52.96 | 50.42 | 51.09 | 53.65 | 50.74 |
| $P_2O_5$ | 40.56 | 39.02 | 36.30 | 40.86 | 39.37 | 42.17 | 41.09 | 41.23 | 41.17 | 41.72 | 39.16 | 40.06 | 42.01 | 40.93 |
| $SiO_2$ | 0.94 | 1.71 | 3.21 | 0.82 | 1.52 | 0.36 | 0.80 | 0.70 | 1.02 | 0.62 | 1.69 | 1.00 | 0.70 | 0.70 |
| FeO* | 0.24 | 0.13 | 0.41 | 0.32 | 0.23 | 0.04 | 0.04 | 0.00 | 0.07 | 0.07 | 0.39 | 0.05 | 0.12 | 0.17 |
| MnO | n.d. | n.d. | 0.00 | 0.00 | n.d. | 0.05 | 0.03 | 0.00 | 0.05 | n.d. | n.d. | n.d. | n.d. | n.d. |
| SrO | 1.66 | 1.56 | 1.04 | 2.69 | 2.46 | 0.08 | 0.11 | 0.03 | 0.06 | 0.04 | 0.04 | 0.14 | 0.95 | 1.11 |
| $Na_2O$ | 0.27 | 0.23 | n.d. | n.d. | 0.04 | n.d. | n.d. | n.d. | n.d. | 0.16 | 0.27 | 0.28 | 0.01 | 0.47 |
| $La_2O_3$ | 1.12 | 1.59 | 2.80 | 0.85 | 1.44 | 0.05 | 0.41 | 0.49 | 0.17 | 0.43 | 1.28 | 0.85 | 0.07 | 1.17 |
| $Ce_2O_3$ | 1.63 | 2.42 | 4.22 | 1.04 | 1.76 | 0.23 | 0.97 | 1.03 | 0.45 | 0.93 | 2.75 | 1.79 | 0.12 | 2.20 |
| $Pr_2O_3$ | 0.08 | 0.21 | 0.27 | 0.03 | 0.08 | 0.04 | 0.19 | 0.13 | 0.10 | 0.17 | 0.19 | 0.18 | 0.10 | 0.19 |
| $Nd_2O_3$ | 0.63 | 0.89 | 1.43 | 0.25 | 0.55 | 0.12 | 0.40 | 0.52 | 0.37 | 0.55 | 1.06 | 0.89 | 0.10 | 0.85 |
| $Sm_2O_3$ | 0.15 | 0.13 | 0.25 | 0.10 | 0.02 | 0.03 | 0.09 | 0.12 | 0.11 | 0.16 | 0.09 | 0.28 | 0.12 | 0.04 |
| $Y_2O_3$ | 0.08 | 0.20 | n.d. | n.d. | 0.01 | n.d. | n.d. | n.d. | n.d. | 0.14 | 0.31 | 0.17 | 0.00 | 0.13 |
| Cl | 0.01 | 0.01 | 0.00 | 0.01 | 0.02 | 0.25 | 0.01 | 0.02 | 0.00 | 0.00 | 0.00 | 0.02 | 0.01 | 0.01 |
| F | 3.40 | 3.39 | 3.98 | 3.44 | 3.68 | 3.06 | 3.38 | 3.84 | 3.85 | 3.65 | 3.84 | 3.66 | 3.68 | 3.91 |
| $-O \equiv F, Cl$ | 1.43 | 1.43 | 1.68 | 1.45 | 1.55 | 1.34 | 1.42 | 1.62 | 1.62 | 1.54 | 1.62 | 1.54 | 1.55 | 1.65 |
| Total | 99.81 | 99.84 | 100.23 | 100.80 | 100.18 | 100.27 | 99.99 | 100.70 | 100.14 | 100.05 | 99.88 | 98.90 | 100.09 | 100.97 |
| Atomic proportions on the basis of 25 oxygens | | | | | | | | | | | | | | |
| P | 5.91 | 5.76 | 5.47 | 5.89 | 5.77 | 5.97 | 5.89 | 5.90 | 5.88 | 5.98 | 5.76 | 5.88 | 5.98 | 5.93 |
| Si | 0.16 | 0.30 | 0.57 | 0.14 | 0.26 | 0.06 | 0.14 | 0.12 | 0.17 | 0.10 | 0.29 | 0.17 | 0.12 | 0.12 |
| Ca | 9.31 | 9.30 | 9.15 | 9.46 | 9.39 | 9.88 | 9.78 | 9.81 | 9.82 | 9.60 | 9.39 | 9.50 | 9.66 | 9.30 |
| Fe | 0.04 | 0.02 | 0.06 | 0.05 | 0.03 | 0.01 | 0.01 | 0.00 | 0.01 | 0.01 | 0.06 | 0.01 | 0.02 | 0.02 |
| Mn | – | – | 0.00 | 0.00 | – | 0.01 | 0.00 | 0.00 | 0.01 | – | – | – | – | – |
| Na | 0.05 | 0.04 | – | – | 0.01 | – | – | – | – | 0.03 | 0.05 | 0.05 | 0.00 | 0.08 |
| Sr | 0.17 | 0.16 | 0.11 | 0.27 | 0.25 | 0.01 | 0.01 | 0.00 | 0.01 | 0.00 | 0.00 | 0.01 | 0.09 | 0.11 |
| La | 0.07 | 0.10 | 0.18 | 0.05 | 0.09 | 0.00 | 0.03 | 0.03 | 0.01 | 0.03 | 0.08 | 0.05 | 0.00 | 0.07 |
| Ce | 0.10 | 0.15 | 0.27 | 0.07 | 0.11 | 0.01 | 0.06 | 0.06 | 0.03 | 0.06 | 0.17 | 0.11 | 0.01 | 0.14 |
| Pr | 0.01 | 0.01 | 0.02 | 0.00 | 0.00 | 0.00 | 0.01 | 0.01 | 0.01 | 0.01 | 0.01 | 0.01 | 0.01 | 0.01 |
| Nd | 0.04 | 0.06 | 0.09 | 0.02 | 0.03 | 0.01 | 0.02 | 0.03 | 0.02 | 0.03 | 0.07 | 0.06 | 0.01 | 0.05 |
| Sm | 0.01 | 0.01 | 0.02 | 0.01 | 0.00 | 0.00 | 0.01 | 0.01 | 0.01 | 0.01 | 0.01 | 0.02 | 0.01 | 0.00 |
| Y | 0.01 | 0.02 | – | – | 0.00 | – | – | – | – | 0.01 | 0.03 | 0.02 | 0.00 | 0.01 |

* Total iron is quoted as FeO. n.d. = not determined

Sample numbers DAR65, DAR67 – quartzite apatites; DAR164, DAR165, DAR167 granite-gneiss apatites; DAR278 – syenite apatites; DAR301 – basalt apatites

c = core; ir = inner rim; or = outer rim of crystal

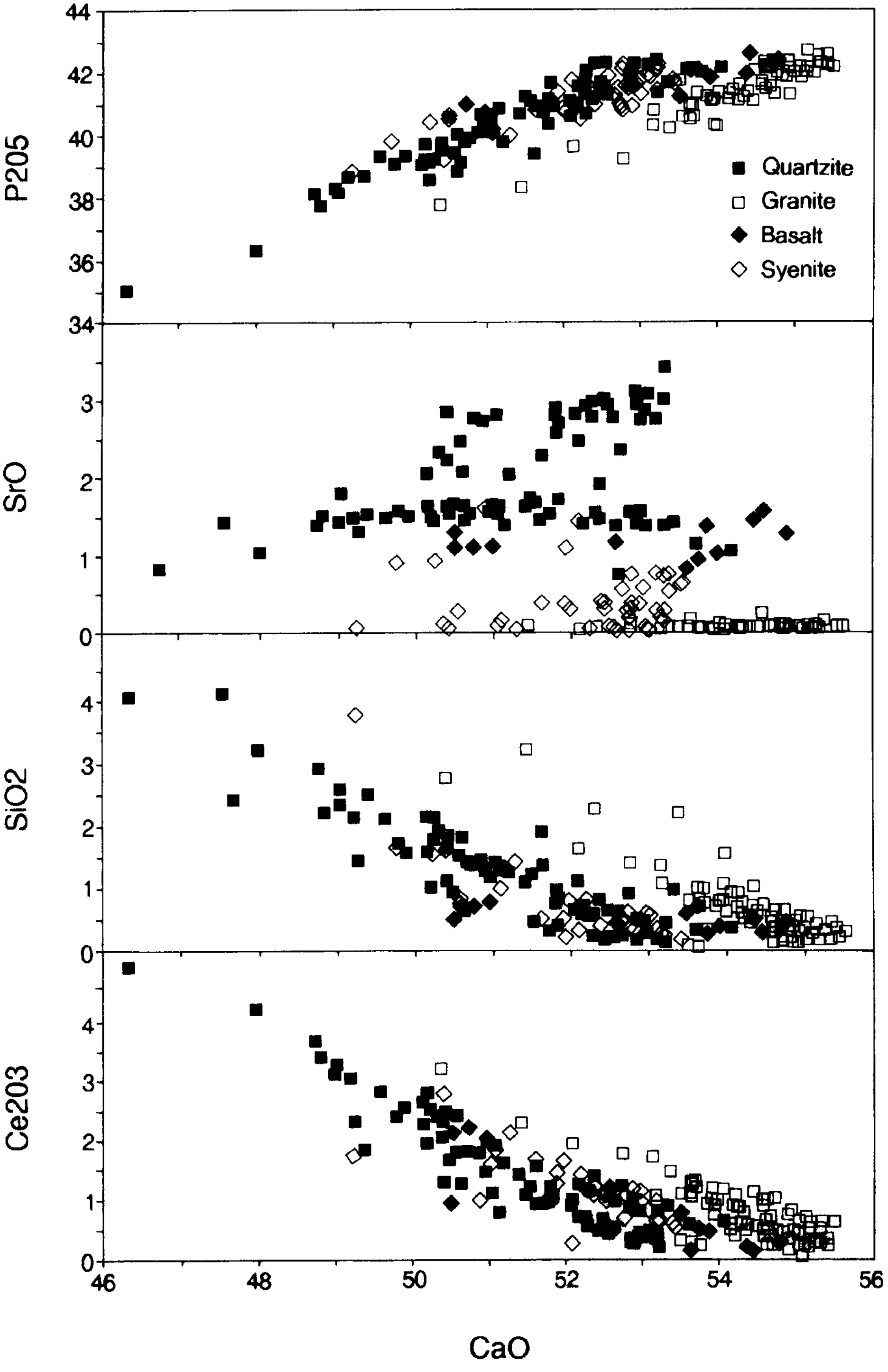

FIG. 4. Selected element variation in the North Qôroq apatites plotted against CaO. The symbols are the same for all plots, and all scales are in oxide wt%.

many analyses for F lie close to the theoretical maximum for this mineral (~3.8 wt.%). Indeed, a number of analyses exceed this value and similar high F values have been reported for apatites from the nearby Ilímaussaq intrusion (Rønsbo, 1989). Such high F determinations need to be critically examined. A number of workers have suggested that $CO_3^{2-}$ can substitute for $PO_4^{3-}$ with the charge balanced by the incorporation of 'excess' $F^-$. A recent discussion of this is given by McArthur (1990). The North Qôroq apatites discussed in this paper do show negative correlation of $P_2O_5$ with F and it is possible that the excess F is due to the substitution outlined above.

Analytical error due to interferences of higher order P-$K\alpha$ lines was avoided as indicated earlier but Stormer *et al.* (1993) have shown that variation in F (and Cl) X-ray intensity can occur due to diffusion of F to the surface of the specimen on exposure to the electron beam. This results in X-ray intensities that vary both with time and the orientation of the apatite. Despite the fact that analyses of the Durango apatite standard produced close to the recommended values for F, it is felt that the F analyses given in Table 1 must be treated with some caution. No attempt is made to calculate variables such as $f_{HF}$ based on these analyses.

Chlorine values for the apatites are generally low, often below detection limits. The exception is apatite from the granite-gneiss whose Cl values reach 0.4 wt.%, much higher than from the other rock types. The highest value is present in apatite from the least altered sample and this suggests that they may originally have been more Cl-rich.

## Discussion

### *Origin of the apatites*

One of the most obvious contrasts in the apatites from in and around the North Qôroq syenites is the Sr contents (Fig. 4). Apatites from the basement granite-gneiss contain virtually no Sr whereas values of 1 to 3 wt.% SrO are typical of those from the quartzite raft. Those from the syenites and basalt samples display variable contents. The other contrast between granite-gneiss apatites and others is the Cl content, which is only significant in the granite-gneiss and appears highest in the least metasomatised rocks. It is proposed that the apatites in the basement gneiss were present as original low-Sr, low-*REE*, chlor/hydroxy-apatites which were modified by later metasomatism, with significant introduction of $F^-$ for $Cl^-$ and $OH^-$ and some introduction of *REE* particularly in the purple luminescing, *REE*-rich rims. Only minor $Sr^{2+}$ was introduced and indeed, Sr from the fluid may have been locked into the plagioclase that occurs in this rock.

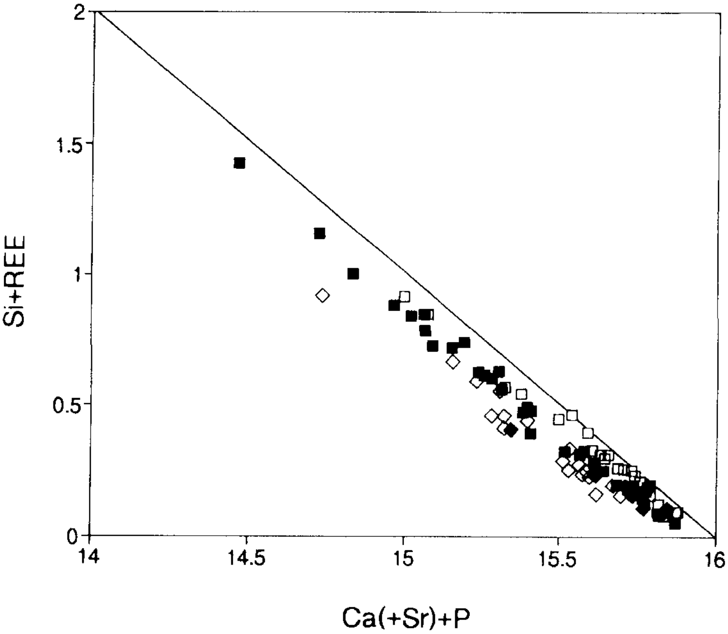

FIG. 5. Rare-earth element substitution in North Qôroq apatites. The symbols are as Fig. 4. Axes are plotted in cations per formula unit. The line on the diagram represents the ideal substitution $Ca^{2+}$ ($Sr^{2+}$) + $P^{5+}$ $\leftrightharpoons$ $REE^{3+}$ + $Si^{4+}$.

In contrast, the Sr-bearing *REE* fluor-apatites from the quartzite raft, so abundant in some areas, are thought to be primary metasomatic in origin. Apatites from the syenites and basaltic supracrustal rocks are likely to contain a mixture of both modified primary and metasomatic apatites. Absence of zoning, or sector zoning, seen in some syenite apatites suggests primary magmatic formation. Such samples occur away from younger syenite units from which fluids would have emanated producing metasomatic replacement and overgrowths.

### *Nature of the fluid*

The extensive *REE* enrichment shows that the fluids responsible for this metasomatism must have been able to transport significant quantities of these elements together with other so called immobile elements (e.g. Zr, Nb). There is abundant experimental and geological evidence concerning the transport and concentration of the *REE* in various systems (e.g. Gieré, 1993; Rubin *et al.*, 1993). Mineyev (1963) shows that the *REE* must be transported in the form of complexes because ionic compounds of the *REE* have very similar chemical properties and so transport in this form would not lead to the fractionation observed in nature. Kosterin (1959) and Ganeyev (1962) noted that high concentrations of the *REE* are associated with high concentrations of alkalis and volatiles and with complexing elements such as Al, $Fe^{3+}$ and Zr, indicating their simultaneous presence in the solution. Alderton *et al.* (1980) showed that the presence of fluoride significantly increases the mobility of the *REE* and Kosterin (1959) favoured the transport of the *REE* by fluor-carbonate complexes in alkaline and oxidising fluids. Wood (1990), on the basis of theoretical predictions, demonstrated that carbonate and fluoride complexes are the most likely forms in which *REE* would be transported in hydrothermal systems at temperatures of <300°C. The close association of apatite with calcite, fluorite, and fluor-carbonate *REE* minerals supports this theory and it is proposed that the bulk of the *REE* in North Qôroq were transported in such complexes. Taylor *et al.* (1981) favour a similar scheme for *REE* enrichment in the peralkaline granites of the Topsails complex, Newfoundland.

The F-rich nature of the fluid phase would produce the fluor-apatites observed, although it should be noted that Korzhinskiy (1981) showed that to obtain $X_{Cl}/X_F = 1$ in apatite at 600°C and 1 kbar the $f_{HCl}$ must be 170 times greater than $f_{HF}$ in the fluid.

The question arises as to whether the F-contents of apatites can be reset by later fluid activity. Several workers note that, while biotite is susceptible to late-stage exchange in the hydroxyl site involving low temperature aqueous fluids, apatite appears to resist this process (Stormer and Carmichael, 1971; Nash, 1976). It appears that while chlor-apatite will exchange and possibly reach equilibrium with a F-rich solution, as may have been the case with the granite-gneiss, fluor-apatite will not react with a Cl-rich solution.

A notable contrast between metasomatic apatites of North Qôroq and the apatites described from Ilímaussaq and other Gardar centres is the lack of any significant substitution of the type $2Ca^{2+} \leftrightharpoons Na^+ + REE^{3+}$. It is tempting to suggest that the substitution of the type $Ca^{2+} + P^{5+} \leftrightharpoons REE^{3+} + Si^{4+}$, dominant in North Qôroq is a reflection of a high activity of silica with both the granite-gneiss and quartzite containing free quartz. However, both the basaltic country rocks and the metasomatised silica-poor, feldspathoidal syenites also show a lack of Na-enrichment in the apatites. Rønsbo (1989) writing on apatites from Ilímaussaq found that the $2Ca^{2+} \leftrightharpoons Na^+ + REE^{3+}$ substitution was most prevalent in a quartz-bearing peralkaline pegmatite, where the apatites were virtually silica free. He suggested peralkalinity as the controlling factor with the substitution involving Na only occurring in highly peralkaline (high $a_{Na_2O}$) environments. North Qôroq syenites evolved to peralkaline (persodic) residua, but not as peralkaline as Ilímaussaq. More importantly, fluids responsible for the *REE* transport would be of very different composition from the silicate magma. The abundant fluorite and carbonate and the presence of calcic pyroxenes, amphiboles and hydro-grossular garnet suggest that the fluid was Ca-rich and Na-poor. Metasomatic alteration by such a fluid would not result in exchange involving Na.

### *Contrasting fluids*

Petrographic and mineral chemistry data suggest quite clearly that metasomatic alteration in and around North Qôroq resulted from the action of two fluids of contrasting composition and that the fluid described above and responsible for *REE* transport was one of these. Both in the quartzite raft and granite-gneiss there are highly metasomatised areas showing albitization and the development of strongly sodic mafic phases. These areas are apatite free and apatite concentrates in veins and patches involving Ca-rich mafic phases, carbonate and fluorite. Similar Ca-rich associations occur in the basalt and are distinct from the general biotite alteration. In both cases the fluid responsible for apatite formation appears to vein and overprint the earlier changes.

Experimental evidence (e.g. Burnham, 1967; Wendlandt and Harrison, 1979) have shown that chloride will partition into the vapour phase and fluoride into the melt in the late-stage crystallization of a felsic magma. Also the *REE* do not partition favourably into aqueous vapour phases at low pressures and therefore will partition preferentially into the melt. This implies that the *REE* will be concentrated into the final magmatic residuum with fluorine, while a chloride-rich vapour phase could separate from the magma at an earlier stage.

It is likely that such a vapour phase was responsible for extensive alkali-metasomatism, but not for *REE* transport or apatite formation. Later, with the continued evolution in the interior of syenitic units, a $F^-$ and $CO_3^{2-}$-rich fluid evolved. As it moved through the pre-existing rocks, altering them, the aggressive nature of this fluid resulted in solution of pre-existing minerals. In the quartzite raft for example, the pods and veins rich in mafic minerals, calcite and apatite may well have resulted from solution of quartz and later infilling caused by the fluid phase.

### *Multiple events*

One of the most interesting features of the metasomatised syenites, granite-gneiss and supracrustal rocks (basalts and quartzite) is the often complex zonation seen in the apatites.

The apatites from the granite-gneiss mainly display simple zonation with irregular *REE*-enriched rims. This has been interpreted as modification to original magmatic apatites in the granite-gneiss, caused by the introduction of fluids rich in *REE* infiltrating the granite-gneiss envelope. Diffusion of *REE*, F and Si from the fluid into the existing chlorapatites occurs and modifies the original composition. The single *REE*-enriched rim is simply a function of the position of the samples, close to only a single syenite unit and hence only subject to a single metasomatic event.

In contrast, complex irregular zoning is developed in the metasomatised syenite and quartzite raft (Fig. 3). Each zone is internally homogeneous and the complex and chaotic sequence of zones shown by a single crystal probably reflects the proximity of samples to several younger syenite units. From each there may have evolved a *REE*-bearing fluid responsible for metasomatism. The differing *REE* concentration in the zones as seen by the contrasting colours in CL and the contrasting brightness of the BSE image reflects distance from their source with *REE* dilution resulting from earlier reactions during the migration of the fluid.

## Conclusions

A study of the apatite chemistry in and around the North Qôroq centre has resulted in the following conclusions relevant to the metasomatising process and *REE* behaviour.

1. The dominant substitution affecting the metasomatic apatites of North Qôroq is $Ca^{2+} + P^{5+} \leftrightharpoons REE^{3+} + Si^{4+}$. The lack of any substitution involving $Na^+$ is probably due to the low peralkalinity or more specifically the low activity of Na in the relevant metasomatising fluid. High activity of silica may also play a part in the granite-gneiss and quartzite in promoting the substitution.
2. The fluid responsible for the *REE* mobility would appear to be $F^-$- and $CO_3^{2-}$-rich, evolving from individual syenite units at a late stage. In addition to apatite formation it results in crystallization of a number of Ca-bearing phases.
3. Metasomatism in North Qôroq results not only from the activity of the fluid described above, but also from the activity of a Cl-, alkali-rich phase evolving from syenitic magmas at an earlier stage. The effects of this may be overprinted by the later $F^-$, $CO_3^{2-}$ fluid activity.
4. Irregular multiple zones in apatite result from multiple metasomatic events with the number and intensity of these directly related to the proximity of the source for each fluid emanation.

## Acknowledgements

Original fieldwork on the North Qôroq centre was supported by Grønlands Geologiske Undersøgelse, and this paper appears by permission of the Director. Research for the current work was carried out during tenure of postgraduate studentships from NERC (GT4/93/110/G, IMC and GT4/85/GS/5, DAR). Valuable assistance with electron micro-probe analyses was given by P.G. Hill, S. Kearns and J. Craven at The University of Edinburgh.

## References

Alderton, D.H.M., Pearce, J.A. and Potts, P.J. (1980) Rare earth element mobility during granite alteration: evidence from south-west England. *Earth Planet. Sci. Lett.*, **49**, 149–65.

Blaxland, A.B., van Breemen, O., Emeleus, C.H. and Anderson, J.G. (1978) Age and origin of the major syenite centres in the Gardar province of South Greenland: Rb-Sr studies. *Geol. Soc. Amer. Bull.*, **89**, 231–44.

Burnham, C.W. (1967) Hydrothermal fluids at the magmatic stage. In *Geochemistry of hydrothermal ore deposits*. (H.L. Barnes, ed.). Holt, Rinehart and Winston (34–76).

Emeleus, C.H. and Harry, W.T. (1970) The Igaliko Nepheline syenite complex: general description. *Meddr. Grønland*, **186**: 3, 115pp.

Filippelli, G.M. and Delaney, M.L. (1993) The effects of manganese (II) and iron (II) on the cathodoluminescence signal in synthetic apatite. *J. Sed. Petrol.*, **63**, 167–73.

Finch, A.A. (1990) *The Chemical and Isotopic Nature of Fluids Associated with Alkaline Magmatism, South Greenland.* Ph.D. thesis, University of Edinburgh, Edinburgh, Scotland.

Ganeyev, I.G. (1962) On the possible transport of matter in the form of complicated complex compounds. *Geochemistry,* **10**, 1042–9.

Gieré, R. (1993) Transport and deposition of *REE* in $H_2S$-rich fluids: evidence from accessory mineral assemblages. *Chem. Geol.*, **110**, 251–68.

Hayward, C.L. and Jones, A.P. (1991) Cathodoluminescence petrography of Middle Proterozoic extrusive carbonatite from Qasiarsuk, South Greenland. *Mineral. Mag.*, **55**, 591–603.

Henderson, P. (1980) Rare earth element partition between sphene, apatite and other coexisting minerals of the Kangerdlugssuaq, E. Greenland. *Contrib. Mineral. Petrol.*, **72**, 81–5.

Korzhinskiy, M.A. (1981) Apatite solid solutions as indicators of the fugacity of HCl° and HF° in hydrothermal solutions. *Geokhimiya,* **18**, 689–706 (in Russian). Translated as *Geochem. Int.*, **18**, 44–60.

Kosterin, A.V. (1959) The possible modes of transport of the rare earths by hydrothermal solutions. *Geochemistry,* **4**, 381–7.

Lieftink, D.J., Nijland, T.G. and Maijer, C. (1994) The behavior of rare-earth elements in high-temperature Cl-bearing aqueous fluids: results from the Ødegårdens Verk natural laboratory. *Can. Mineral.*, **32**, 149–58.

Macdonald, R. and Upton, B.G.J. (1993) The Proterozoic Gardar rift zone, south Greenland: comparisons with the East African Rift System. In *Magmatic Processes and Plate Tectonics.* (H.M. Prichard, T. Alabaster, N.B.W. Harris and C.R. Neary, eds.). *Spec. Publ. Geol. Soc., London No.* **76**, 427–42.

Mariano, A.N. and Ring, P.J. (1975) Europium-activated cathodoluminescence in minerals. *Geochim. Cosmochim. Acta,* **39**, 649–60.

Marshall, D.J. (1988) *Cathodoluminescence of Geological Materials*, Unwin Hyman, London.

McArthur, J.M. (1990) Fluorine-deficient apatite. *Mineral. Mag.*, **54**, 508–10.

McConnell, D. (1973) *Apatite: its crystal chemistry, utilization and geologic and biologic occurrences.* New York: Springer-Verlag.

Mineyev, D.A. (1963) Geochemical differentiation of the rare earths. *Geochemistry,* **12**, 1129–49.

Nash, W.P. (1976) Fluorine, chlorine and OH-bearing minerals in the Skaergaard intrusion. *Amer. J. Sci.*, **276**, 546–57.

Palilla, F.C. and O'Reilly, B.E. (1968) Alkaline-earth halophosphate phosphors activated by divalent europium. *J. Electrochem. Soc.*, **115**, 1076–81.

Portnov, A.M. and Gorobets, B.S. (1969) Luminescence of apatite from different rock types. *Dokl. Akad. Nauk. SSSR,* **184**, 199–202 (in Russian).

Quirk, R. and Thomas, M.J.B. (1964) Effect of composition and structure of halophosphate phosphors on color of fluorescence. *Electrochem. Soc. Abstr.*, **13**, 32–3.

Reed, S.J.B. (1986) Ion microprobe determination of rare earth elements in accessory minerals. *Mineral. Mag.*, **50**, 3–15.

Roeder, P.L., MacArthur, D., Ma, X.-P., Palmer, G.R. and Mariano, A.N. (1987) Cathodoluminescence and microprobe study of rare-earth elements in apatite. *Amer. Mineral.*, **72**, 801–11.

Rønsbo, J.G., Khomyakov, A.P., Semenov, E.I., Voronkov, A.A. and Garanin, V.K. (1979) Vitusite — a new phosphate of sodium and rare-earths from the Lovozero alkaline massif, Kola, and the Ilímaussaq alkaline intrusion, South Greenland. *Neues Jahrb. Mineral. Abh.*, **137**, 42–53.

Rønsbo, J.G. (1989) Coupled substitutions involving *REE*s and Na and Si in apatites in alkaline rocks from the Ilímaussaq intrusion, South Greenland, and the petrological implications. *Amer. Mineral.*, **74**, 896–901.

Rubin, J.N., Henry, C.D. and Price, J.G. (1993) The mobility of zirconium and other 'immobile' elements during hydrothermal alteration. *Chem. Geol.*, **110**, 29–47.

Smith, J.V. and Steenstrom, R.C. (1965) Electron-excited luminescence as a petrologic tool. *J. Geol.*, **73**, 627–35.

Steiger, R.H. and Jäger, E. (1977) Subcommission on geochronology: convention on the use of decay constants in geo- and cosmochronology. *Earth Planet. Sci. Lett.*, **36**, 359–62.

Stormer, J.C. and Carmichael, I.S.E. (1971) Fluorine-hydroxyl exchange in apatite and biotite: a potential igneous geothermometer. *Contrib. Mineral. Petrol.*, **31**, 121–31.

Stormer, J.C. Jr., Pierson, M.L. and Tacker, R.C. (1993) Variation in F and Cl X-ray intensity due to anisotropic diffusion in apatite during electron microprobe analysis. *Amer. Mineral.*, **78**, 641–8.

Taylor, R.P., Strong, D.F. and Fryer, B.J. (1981) Volatile control of contrasting trace element distributions in peralkaline granitic and volcanic rocks. *Contrib. Mineral. Petrol.*, **77**, 267–71.

Upton, B.G.J. and Emeleus, C.H. (1987) Mid Proterozoic alkaline magmatism in southern Greenland. In *Alkaline Igneous Rocks.* (J.G. Fitton and B.G.J. Upton, eds.). *Spec. Publ. Geol. Soc., London,* **30**, 449–71.

Voron'ko, Y.K., Gorbachev, A.V., Zverev, A.A., Sobol', A.A., Morozov, N.N., Murav'ev, E.N., Niyazov, S.A. and Orlovskii, V.P. (1992) Raman scattering and luminescence spectra of compounds with the structure of apatite $Ca_5(PO_4)_3F$ and $Ca_5(PO_4)_3OH$ activated with $Eu^{3+}$ ions. *Neorganicheskie Materialy,* **28**, 582–9 (in Russian). Translated as: *Inorganic Materials,* **28**, 442–7.

Walker, G. (1985) Mineralogical applications of luminescence techniques. In *Chemical bonding and spectroscopy in mineral chemistry* (F.J. Berry and D.J. Vaughan, eds.). Chapman and Hall, London (103–40).

Watson, E.B. and Green, T.H. (1981) Apatite/liquid partition coefficients for the rare earth elements and strontium. *Earth Planet. Sci. Lett.,* **56**, 405–21.

Wendlandt, R.F. and Harrison, W.J. (1979) Rare earth partitioning between immiscible carbonate and silicate liquids and $CO_2$ vapor: results and implications for the formation of light rare earth-enriched rocks. *Contrib. Mineral. Petrol.,* 69, 409–19.

Wood, S.A. (1990) The aqueous geochemistry of rare elements and Yttrium 2. Theoretical predictions of speciation in hydrothermal solutions to 350°C at saturation vapour pressure. *Chem. Geol.,* **88**, 99–125.

Young, E.J., Myers, A.T., Munson, E.L. and Conklin, N.M. (1969) Mineralogy and geochemistry of fluorapatite from Cerro de Mercado, Durango, Mexico. *U.S. Geol. Surv., Prof. Paper,* **650-D**, 84–93.

[*Revised manuscript received 10 July 1995*]